water

MDPI

Article

Evaluation of Local Scour along the Base of Longitudinal Training Walls

Nelson Javier Cely Calixto [1,2,*], Alberto Galvis Castaño [1] and Gustavo Adolfo Carrillo Soto [2]

[1] Grupo de Investigación en Gestión Integrada del Recurso Hídrico (GIRH), Universidad del Valle, Ciudad Universitaria Meléndez, Calle 13 # 100-00, Cali 760015, Colombia; alberto.galvis@correounivalle.edu.co

[2] Grupo de investigación en Hidrología y Recursos Hídricos (HYDROS), Universidad Francisco de Paula Santander, Av. Gran Colombia, No. 12E-96, Cúcuta 540001, Colombia; gustavocarrillo@ufps.edu.co

* Correspondence: nelson.cely@correounivalle.edu.co

Abstract: This study proposes a new empirical model for estimating local scour along the base of longitudinal training walls for granular riverbeds. The model's performance was rigorously assessed through experiments conducted in an open-channel flume, encompassing variations in granulometric characteristics, slope, and flow rates. The investigation involved a comparative analysis of six commonly employed equations for scour estimation. The results consistently demonstrated a tendency of the selected equations to overestimate scour depth within the longitudinal structures. In contrast, the new proposed equation considers factors such as the well-graded granular bedding represented by the Coefficient of uniformity (C_u) and the embedment of the longitudinal wall. This allows for a more robust identification of the scour behavior of longitudinal walls. This research enhances our comprehension of local scour in riverbeds. It provides engineers and researchers with a valuable tool for more accurate predictions, thereby contributing to the improved design and maintenance of river environment structures.

Keywords: river bank protection; longitudinal training walls; sediment transport; scour depth estimation

check for updates

Citation: Cely Calixto, N.J.; Galvis Castaño, A.; Carrillo Soto, G.A. Evaluation of Local Scour along the Base of Longitudinal Training Walls. *Water* **2023**, *15*, 4001. https://doi.org/10.3390/w15224001

Academic Editor: Bommanna Krishnappan

Received: 7 October 2023
Revised: 6 November 2023
Accepted: 8 November 2023
Published: 17 November 2023

1. Introduction

As technology and science progress, river courses without human intervention are becoming rare, while different engineering projects focused on improving navigation and reducing flood risks are more commonplace [1]. Scour represents a primary mechanism within the realm of water erosion, whereby it engages in the excavation of bed materials and induces a reduction in the structural integrity of fortifications safeguarding riverbanks or margins [2–4]. These erosional processes are mainly influenced by local scour, a phenomenon where sediment near the surface of the riverbed is rolled up and transported downstream [5].

Longitudinal hydraulic structures, such as retaining walls, are widely used worldwide to protect the conditions that allow the stability of slopes, protecting populations settled along the riverbanks [6] and improving the strength of the cross slopes of the riverbed, which directs the flow to an undulating current. Therefore, the scour analysis of such structures is a critical step to identify possible adverse situations due to turbulent flow and that its foundations are exposed to the action of the stream flows [6,7].

Natural rivers, mainly in areas with little intervention, flow over a bed or sediments deposited by dragging and deposition due to their size and environment. These are called alluvial rivers and present variable granulometric conditions, which vary in gravel composition (with an average diameter of 2 mm), variable percentages of sand (with an average diameter of 0.1 mm), and slopes greater than 0.5% [8,9]. Likewise, they present a Coefficient of uniformity (C_u) greater than 20, which indicates that the sediment is well-graded and homogeneous in composition [10,11].

Various factors influence the scour phenomena, encompassing parameters like flow regime, discharge, sediment dimensions, morphology, channel width, bed slope, flow velocity, and cross-sectional geometry [12,13]; the latter impedes the precise assessment of the utmost scour depth along the foundation of longitudinal structures [14] since a high scour depth increases the instability of the walls, which can cause terrain loss, a change in the river course, a change in the slope, economic loss, and eventually (in a worst-case scenario) human fatalities [15].

Over the years, diverse mathematical expressions to estimate scour have been proposed. These approximations are used in modern-day engineering; however, to the author's knowledge, they have not been validated for well-graded granular bedding. Most of these equations are based on physical models with scour conditions in clear water (where there is no sediment transport toward the structure). This condition mainly occurs on thick riverbeds and is helpful for experimentation, enabling a reliable calculation of the maximum scour depth [16]. In hydraulic structures, general scour is often analyzed considering the physical components of contraction, as it often becomes the leading cause of erosion due to increased streambed material's drag in the flow's cross-section and changes in the flow regime [17].

The equations for general scour presented by Blench [18] and by Lacey [17] were initially developed to use a system of specific units. Later, Lischtvan and Lebediev [19] proposed a new method that uses dimensionless variables by adding the contraction variable. Other methods are available to estimate this phenomenon, such as those presented by several authors [20,21]. These mathematical expressions commonly analyze streambed material size and the riverbed width. Nonetheless, only Laursen and Toch [20] consider sediment transport, while Komura [22] explicitly considers flow velocity. Recently, Khosronejad et al. [14] developed an equation that evaluates the river's sinuosity to predict scour in curved vertical walls. Mathematical expressions for calculating local scour were developed to estimate the scour development, especially in bridge abutments and piers or spurs. Also, these equations are frequently used to analyze longitudinal walls [23]. In contrast, other equations consider the shape of the abutment without the tilt angle, which is better for the case of longitudinal walls [24–27]. Finally, authors such as Khosronejad et al. [14] and Mussetter et al. [28] consider the tilt, enhancing the prediction of those structures.

Over the years, several authors have proposed different approaches for calculating maximum scour depth in longitudinal structures despite considering almost the same condition for granular bedding. The main problem of scouring in longitudinal walls has not been thoroughly studied compared to scouring on bridge abutments. The latter can be observed when considering the few specific estimation methods for scouring walls. Although the equations that can predict scour in abutments are applied to walls, there is still no mathematical relation to estimating the maximum scour depth for longitudinal walls in rivers with well-graded granular bedding and embedded walls. Hence, there is uncertainty in engineering designs of longitudinal walls, as there can be a lack of consideration of relevant parameters (geometric, hydraulic, or geotechnical) or the possibility of being outside the application ranges in specific conditions [14,28]. The current equations for predicting maximum scour depth in longitudinal structures do not consider wall embeddedness, which can influence how vortices are produced and, thus, create greater local scour [17]. The case of the equation described by Mussetter et al. [28] considers wall thickness, which makes a shock in the flow at the structure's entrance, generating local scour at the initial point, which can be reduced by embedding the wall into the riverbanks. In practice, this embedding minimizes the vortices caused by the shock at the wall's entrance. However, the authors did not initially assess further details on the specific information about the produced scour.

The main objective of this research is to propose a new mathematical expression for estimating the local scour depth in longitudinal walls in rivers with well-graded granular bedding, using physical modeling in a channel with certain conditions of fixed bedding, slope, and flow rate.

2. Materials and Methods

2.1. Experimental Setup

The experiments were conducted at the Laboratory of Experimental Hydraulics of Universidad Santo Tomás (Tunja, Colombia). A 5 m × 0.3 m × 0.4 m (length, width, and depth, respectively) laboratory-scale experimental flume (HM 162, G.U.N.T. Gerätebau GmbH, Hamburg, Germany) with a closed flow circuit was used for the different experiments (Figure 1a). Various flow conditions (0.008, 0.017, 0.025, and 0.030 m^3/s) and different slopes (0.5 and 2.5%) were analyzed to determine the changes in the maximum scour depth. Eleven measurement points were located along the experimental flume (Figure 1b). This configuration allowed obtaining information on scour depths from the initial point where the water interacts with the wall to its final edge.

(**a**)

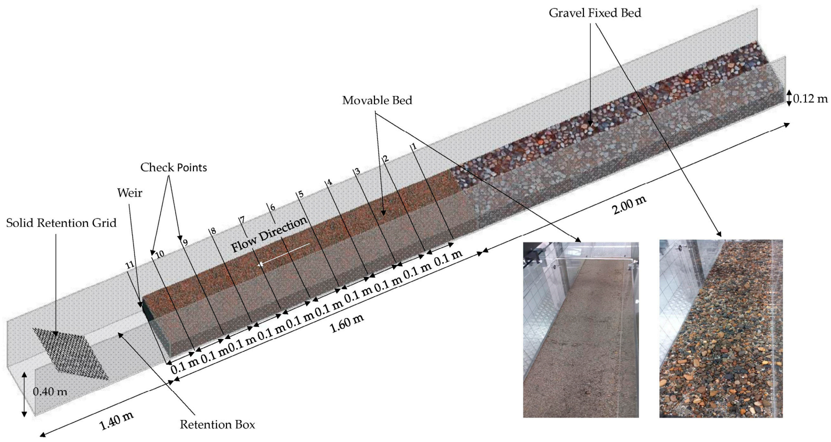

(**b**)

Figure 1. A complete view of the experimental flume (**a**) and the composition of the measurement points (**b**).

According to Look [29] and Sotiropoulos and Diplas [14], it is recommended that the longitudinal protection walls should be embedded within the lateral slope of the channel in order not to contract the width of the channel and, therefore, not to generate an obstacle to the flow, which can cause scour by a direct collision of the flow with the beginning of the wall. Thus, the experimental development takes into account this concept of lateral embedment of the wall, and the longitudinal wall is assumed to be the wall of the hydraulic channel used for the experimental development.

2.2. Riverbed Composition

The granulometric curve was constructed by referencing typical river curves characterized by granular beds with mean sediment diameters ranging from 20 to 35 mm and Coefficient of uniformity (C_u) of 24.81 and 24.96, respectively [8,9,30], obtained through the

d_{60}/d_{10} ratio corresponding to diameters for which 60% and 10% of the particles of the soil (in weight) are equal or less between each other. To establish a theoretical granulometric curve for sediments with a mean diameter of 7.75 mm within a well-graded granular bed while ensuring a Coefficient of uniformity (C_u) significant than 20, we performed scaling on the curves derived from actual rivers [31,32]. Additionally, the proportions of each constituent of the bed (fine sand, coarse sand, and gravel) based on the sediment passing through specific laboratory sieves were calculated.

2.3. Equations for Scour Depth Prediction

The most common scour equations were used in this study. These are described as follows:

Equation (1), Lischtvan-Lebediev [19]. The equation is used for cohesionless soils; it considers flow contraction due to the presence of abutments and piers and the specific weight of the water. Consequently, it requires a correction through adjustment factors for bridge evaluation.

$$H_s = \left[\frac{\alpha H^{\frac{5}{3}}}{0.68 \beta D_m{}^{0.28} \varphi} \right]^{\frac{1}{1+z}} \tag{1}$$

where H_s = maximum scour depth (m), H = water depth (m), D_m = average diameter of the riverbed (mm), β = frequency coefficient, which depends on the return period (see Appendix A), φ = Coefficient that depends on the concentration of the transported material (from tables described by Blench [18]), Z = exponent as a function of the average particle diameter, and α = Section coefficient dependent on hydraulic characteristics (see Appendix A).

Equation (2), Mussetter et al. [28]. The equation can be applied to longitudinal walls; it contemplates the maximum amount of scour in angles (α) conditions that vary from 0° to 90° for a flow parallel and perpendicular to the longitudinal wall.

$$\frac{H_s}{H} = \left(0.73 + 0.14\pi Fr^2\right) cos\ \alpha + 4Fr^{\frac{1}{3}}\ sin\ \alpha \tag{2}$$

where H_s = maximum scour depth, H = water depth (m), and Fr = Froude number.

Equation (3), Borges [23]. The equation estimates scour in walls, which considers its thickness and length.

$$\frac{Y_s}{Y_n} = 0.267 Fr^{1.95} \left(\frac{Y_n}{D_{50}}\right)^{0.60} \left(\frac{L}{E}\right)^{-0.09} \tag{3}$$

where Y_s = maximum scour depth (m), Y_n = water depth (m), L = length of the wall (m), E = wall thickness, and D_{50} = average particle size.

Equation (4), Froehlich [26]. The equation estimates scour in a mobile bed as in clear water, for abutments, and a concentrated flow on flooding zones.

$$\frac{H_s}{H} = 2.27 K_f K_\theta \left(\frac{L}{H}\right)^{0.43} F_r{}^{0.61} + 1 \tag{4}$$

where H_s = maximum scour depth, H = water depth, K_f = Coefficient that depends on the shape of the abutment (from tables described in [26]), K_θ = Coefficient that depends on the attack angle of the flow (from tables described in [26]), L = length of the abutment, and F_r = Froude number of the section obstructed by the abutment.

Equation (5), Pereira [33]. The equation estimates local scour in abutments perpendicular to the current and flow conditions higher than critical in curved channels.

$$\frac{H_s}{H_n} = 0.425 Fr^{1.08} \left(\frac{H_n}{D_{50}}\right)^{0.365} \left(\frac{L}{B}\right)^{0.163} \tag{5}$$

where H_s = maximum scour depth, H_n = average flow depth, L = curve length, D_{50} = average particle size, and B = width of the abutment.

Equation (6), Khosronejad et al. [14]. The equation calculates local scour in longitudinal walls for granular material; it evaluates the layout slope of the wall and estimates that an increase in the formed angle decreases the scour.

$$\frac{H_s}{D_{50}} = 1909\langle Fr\widetilde{s}\vartheta\rangle^{\frac{-10}{9}} + \frac{8}{5}Fr_d - \frac{3\pi}{2}e^{(k_s/H)^{1/10}} \quad (6)$$

where H_s = maximum scour depth, $\widetilde{s}$ = sinuosity, ϑ = angle between the longitudinal wall and the shore, D_{50} = average particle size, Fr = Froude number, Fr_d = densimetric Froude number, and k_s = roughness of the bed.

2.4. Statistical Validation

The validation was carried out by comparing the data obtained in the experiments and the current scour equations described above. Mean Normalized Error (MNE), Mean Prediction Factor (MPF), Mean Square Error (MSE), and Root Mean Square Error (RMSE) [31,34], were calculated using SPSS software (IBM Corp. Released 2015. IBM SPSS Statistics for Windows, Version 23.0. Armonk, NY: IBM Corp).

Equation (7), Mean Normalized Error (MNE): The normalized absolute deviation between the expected and the measured data is expressed as a percentage. It has an acceptable maximum value of 200. It is obtained through:

$$MNE = \frac{100}{N}\sum_{i=1}^{N}\frac{|X_{mi} - X_{ci}|}{X_{mi}} \quad (7)$$

where X_{mi} = real data (measured), X_{ci} = theoretical data (calculated), i = initial value, and N = total amount of data.

Equation (8), Mean Prediction Factor (*MPF*), is a statistical indicator used to compare the prediction accuracy of functional relations. With it, the behavior of the data set is shown. The *MPF* has an ideal value equal to 2.

$$MPF = \frac{1}{N}\sum_{i=1}^{N} Max\left(\frac{X_{mi}}{X_{ci}}; \frac{X_{ci}}{X_{mi}}\right) \quad (8)$$

where X_{mi} = real data (measured), X_{ci} = theoretical data (calculated), i = initial value, and N = total amount of data.

Equation (9), Mean Square Error (*MSE*). The mean squared error measures the randomness of the information used to estimate. For this reason, the *MSE* is always positive and not 0. For the *MSE*, the higher the value, the worse the model is. A value of *MSE* = 0 would be a perfect model.

$$MSE = \frac{1}{N}\sum_{i=1}^{N}(\hat{y}_i - y_i)^2 \quad (9)$$

where $\hat{y}_i$ = theoretical data (calculated), y_i = real data (measured), i = initial value, and N = total amount of data.

Equation (10), Root Mean Squared Error (*RMSE*) represents the standard deviation of the residual values of the mean squared error. The residual values measure the variation between the points or data of the regression line. The Root Mean Square Error represents the level of dispersion of the residual values of the *MSE*, i.e., it indicates the concentration of data at the line of best fit.

$$RMSE = \sqrt{MSE} \quad (10)$$

3. Results and Discussion

3.1. Riverbed Composition

Figure 2 shows the Coefficient of Uniformity (C_u) for the granulometric curves. The data showed values between 24.96 and 24.81 with a median diameter of 35.21 and 22.86 mm, respectively. These curves were scaled to generate the theoretical granulometric curve with a C_u of 20.49 and an average diameter of 7.75 mm, obtained through the d_{60}/d_{10} ratio. According to the results, the necessary volumes of fine sand, coarse sand, and gravel were obtained (46, 26, and 28%, respectively).

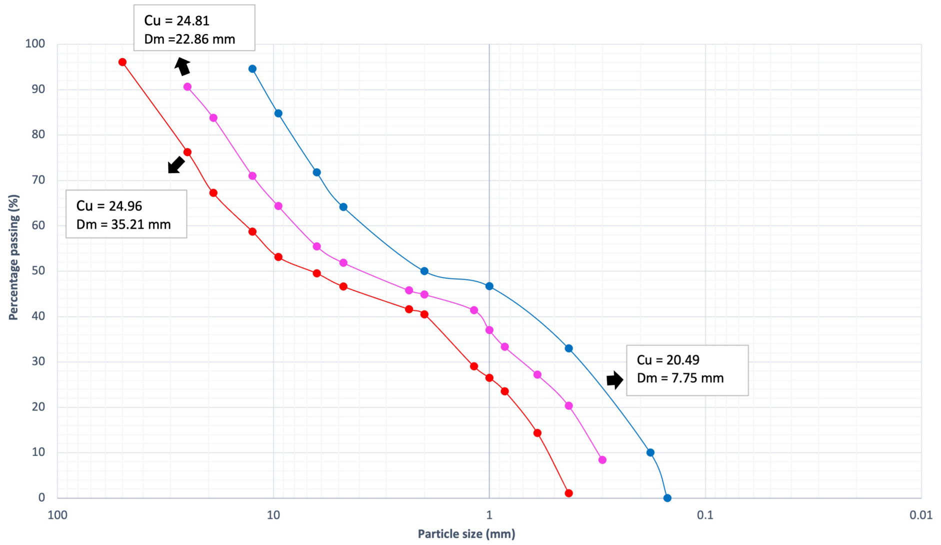

Figure 2. Particle size distribution of the bed materials used in the model.

After 160 min, the start of a constant scour is observed. Another 60 min were added to demonstrate the linearity of the values of maximum scour depth, with an average value of 97 mm up to a maximum value of 97.5 mm in the analysis conducted between 200 and 220 min. With the implemented diameters (Figure 3) and channel depth, the necessary conditions were fulfilled to exclude viscosity and macro roughness effects, which are diameters larger than about 0.9 mm and flow depths above 20 mm [35].

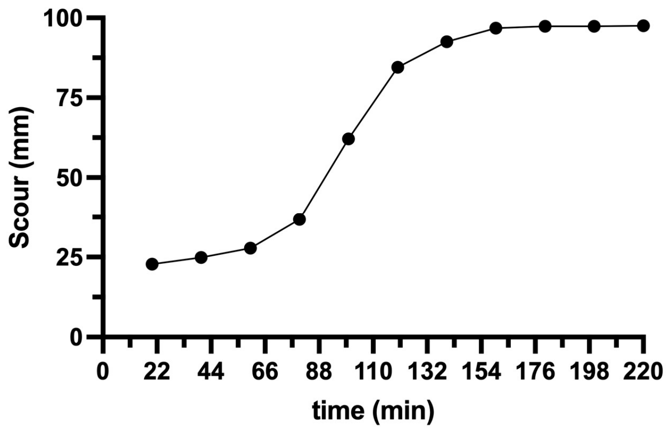

Figure 3. Temporal evolution of maximum scour depth during the preliminary experiment.

3.2. Experimental Results

The present work focuses on the analysis of scour throughout the experimental time, also called "temporal scour evolution"; likewise, the term "equilibrium condition" refers to the maximum scour depth reached throughout the experimental development, which does not show variation throughout the experimental procedure. Twenty experiments were conducted varying the longitudinal slope and the flow rate, considering the typical characteristics of rivers with well-graded granular bedding. Throughout the different experiments, the inlet flow rate was kept constant, which added to the slope, and the clash of the flow against the sediment maintained a turbulent flow during the 220 min of modeling. According to the data obtained (Figure 4), the slope of the channel affects the maximum scour depth, as a greater slope increases the scour depth and creates a removal of sediment from the bottom of the riverbed, mainly in the first checkpoints, due to the shock of the flow at the entrance that drags the sediment [36]. Although there are certain variations in some control points concerning the scour depth, the scour along the longitudinal wall on the left and right sides of the granular bedding behaves similarly in each of the conditions analyzed in the investigation. Therefore, the size of the bed implemented is considered adequate since, as can be seen in the results obtained, the bed arranged does not scour entirely along the entire length of the bed, so it can be inferred that the control or measurement points placed along the bed are sufficient to analyze the behavior of the scour depth for each of the conditions set out in the research.

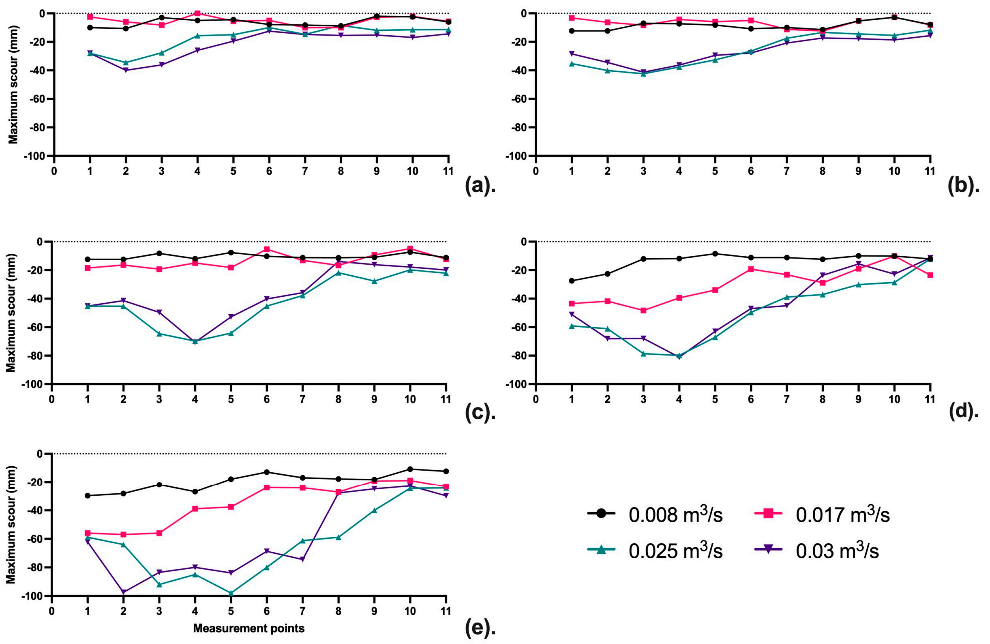

Figure 4. Maximum scour measurements for the eleven control points for different discharges and slope configurations. slope = 0.5% (**a**), slope = 1% (**b**), slope = 1.5% (**c**), slope = 2% (**d**), and slope = 2.5% (**e**).

An increase in the scour depth can also be observed as the flow rate increases (Figure 4). The dreadnought inside the scour bottom is produced by the washing of material and the deposition of particles that are transported from upstream, where due to the diameter of the particles, part of this material cannot be removed by the action of the central vortex that the flow of water presents [23]. In general, the adjustment of the riverbed in each experiment, the dragging, and the decanting of the material in the checkpoints caused the value of the scour depth to not increase despite the flow rate increase.

The channel width (0.3 m) used in the study can be considered sufficient to determine the scour behavior in well-graded granular beds of sands and gravels with a mean diameter of less than 10 mm. The above is consistent with research conducted by Radice and Davari [37] who analyzed roughness elements as a scour countermeasure in pillars, having a 0.4 m wide channel, and introducing additional characteristics that further decrease the section, but which, in turn, do not generate effects on the scour analysis for the conditions evaluated. Similarly, Borges [23] used a 0.45 m wide channel section as a scenario for scour analysis and comparison with that presented in channels with larger cross sections. It can be highlighted that the size of the bed implemented can be considered adequate since, according to the results obtained, the bed does not scour along the entire length of the channel. It was also possible to observe sediment entrainment at the initial points and sediment deposition at the final points, so it can be inferred that the measurement points arranged along the bed and the depth and length are sufficient to analyze the behavior of the scour depth.

In the experiments, the value of maximum scour depth for a slope of 2.5% and discharge of 0.03 m^3/s reached 97.5 mm, observed in the second monitoring point. It is a significantly high value with which the instability of the longitudinal structure occurs. Table 1 compares the average depth change between the lowest proposed slope of 0.5% and the highest (2.5%), where differences that reach 83 mm were obtained. This is a significant difference and we can observe the direct effect of the slope on the maximum scour depth. It should be noted that there was no symmetry in the scour because, along the wall, there was sediment at the beginning of the channel and deposition at the end of it. However, the channel's symmetry does not affect the equation proposed since it depends on the Froude number and the densimetric Froude number, which can vary and be measured at any point of the channel with well-graded granular material.

Table 1. Maximum scour depth (mm) Comparison between maximum (2.5%) and minimum (0.5%) slope.

Slope (%)	Discharge (m^3/s)	Maximum Scour Depth (mm)										
		1	2	3	4	5	6	7	8	9	10	11
0.5	0.008	10	10.6	3	5	4.4	7.8	8.2	8.8	2	2.4	6
	0.017	2.5	6	8.2	0	5.5	5	10	10	2.7	2.1	5.6
	0.025	28	34.5	27.6	15.6	15	10	14.7	8.5	11.9	11.5	11.3
	0.03	28	40	36.1	26	19.5	12.5	14.8	15.5	15.2	16.9	14.4
		1	2	3	4	5	6	7	8	9	10	11
2.5	0.008	29.7	28.2	21.9	26.9	17.9	12.9	16.9	17.7	18.2	10.8	12.3
	0.017	56	57	56	38.9	37.6	23.9	24.1	27.1	19.2	18.9	23.2
	0.025	58.9	64	92	85	98	80	61.2	58.9	40	24.5	24.2
	0.03	62.1	97.5	83.5	80	83.9	68.7	74.5	27.8	24.9	22.8	29.8

3.3. Analysis of Existing Equations Used to Predict Scour

To analyze the equations that predict the maximum scour depth, data from point 4 to point 11 were used. In contrast, values of points 1 to 3 could not be utilized as a hydraulic jump occurs, which means that this depth data do not represent a real scour on the wall due to a natural erosive action of the flow. The maximum value of scour was used as a representative value in the data obtained from sampling points 4 to 11. Atypical data were adjusted through the calculated error to generate theoretical consistency with increased flow rate and slope. In this manner, the final comparative values were obtained and used to ascertain the efficacy of the predictive equations.

Figure 5 compares the predictive equations and the data obtained in the experimental model. The results of equations [14,23] and Mussetter et al. [28] tend to show higher dispersion. On the other hand, among the equations validated in this research, the best adapted to the evaluated variables and conditions is the equation proposed by Lischtvan and Lebediev [19], as it shows a low dispersion, which translates into an accurate prediction of scour in longitudinal walls in rivers with well-graded granular bedding.

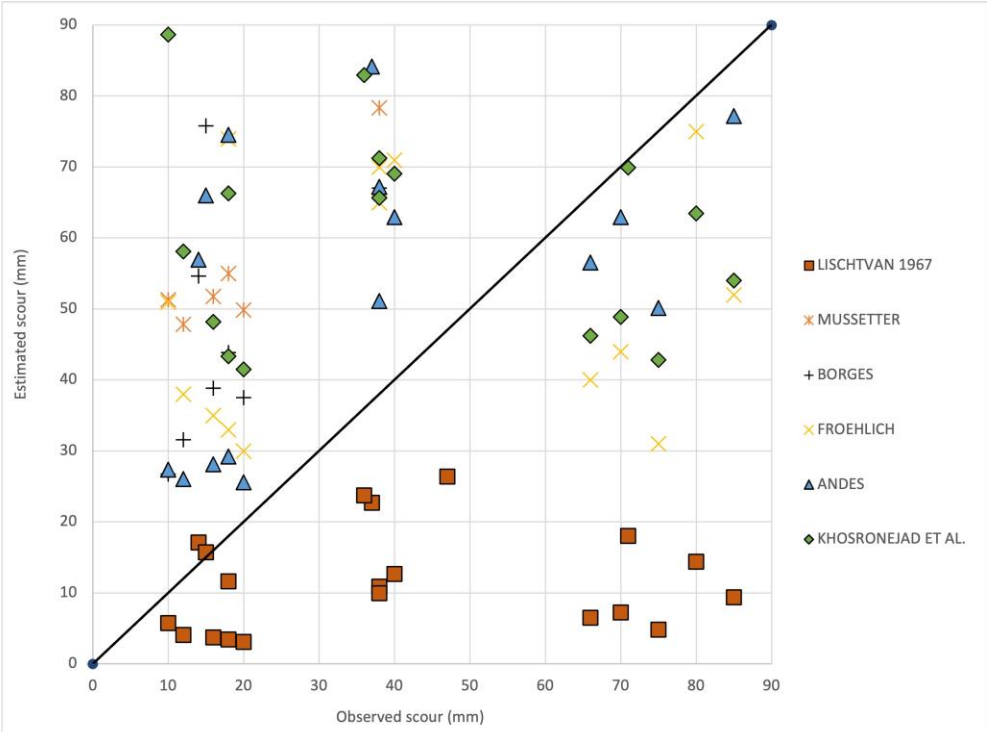

Figure 5. Maximum Scour depth estimation by current equations.

3.4. Development of a New Mathematical Expression to Calculate Local Scour

This paper proposes a new mathematical expression to improve the prediction of scour depth in longitudinal walls in a condition of wall embeddedness and well-graded granular bedding. A dimensional analysis of the variables that influence the physical model was conducted to attain this expression. These were PI numbers and were analyzed according to the relationship between the experimental data obtained for $\frac{H_s}{Y_n}$ where a linear regression model was applied. The data with $r^2 < 0.75$ were discarded and the PI numbers with values close to 1 were used: the Froude number (Fr) and densimetric Froude number (Frd).

With PI numbers, a model of exponential adjustment is created through which values for the coefficients of each variable are obtained. After that, more than 100 mathematical iterations were conducted, from which more than ten different equations to estimate local scour were formulated. These equations were analyzed according to the scour measured through the experiments and a linear regression model for each equation was attained. The equation with an r^2 closest to 1 was selected from the regression models of each equation. Lastly, a new Equation (11) was proposed to estimate the depth of local scour in longitudinal walls in rivers with well-graded granular bedding.

$$\frac{Hs}{Yn} = 0.043 * Frd^{0.643} * F^{2.188} \tag{11}$$

Figure 6 shows the correlation between the observed scour depths and those calculated with the new proposed mathematical expression, which delivered a r^2 of 0.8567.

Figure 7 shows a three-variable diagram depicting the dimensionless relationship among critical variables: the Froude number (Fr), the densimetric Froude number (Frd), and the dependent variable, scour depth (H_s), relative to flow depth (Y_n). This diagram facilitates the calculation of scour depth as a function of the Froude number, which was subsequently validated against experimental data obtained from physical models representing well-graded granular beds and longitudinal structures.

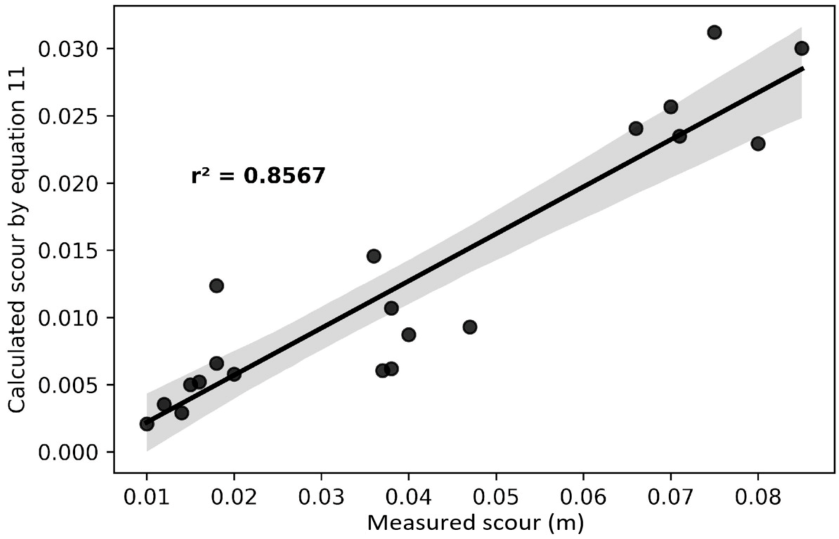

Figure 6. Lineal regression of the results of the proposed equation and the experimental data to estimate the maximum local scour.

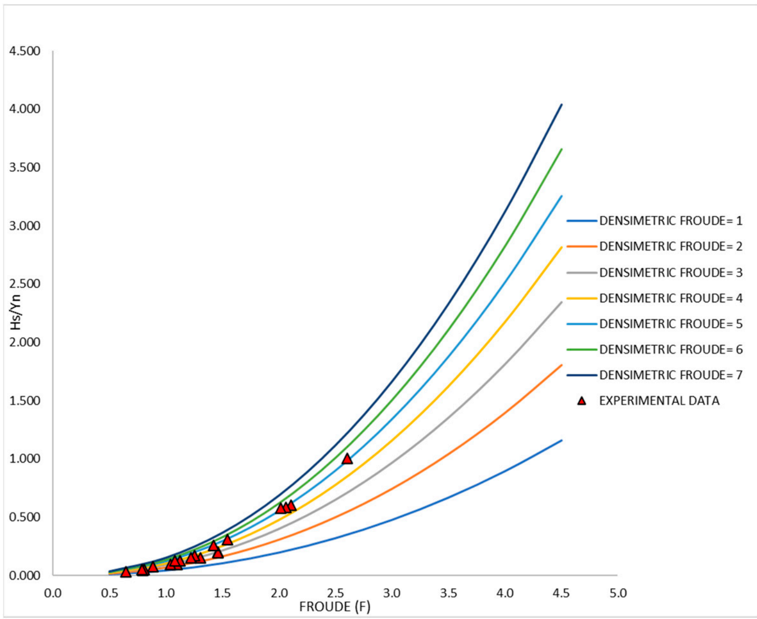

Figure 7. Maximum Scour depth estimation by the prediction equation.

3.5. Validation of the New Mathematical Expression to Calculate the Local Scour

Table 2 shows the statistical analysis for comparing the equations to predict scour. In this analysis, the proposal from Aguirre-Pe et al. [38] was considered and error correction was conducted to establish a maximum acceptable value of 200 for the MNE. The result allowed a representative margin for the proposed mathematical equation to improve the prediction of maximum scour. Data showed that the novel equation obtained an MNE of 68.72%, which was only surpassed by Lischtvan–Lebediev's equation [19] (MNE of 63.03%). Likewise, it can be observed that the equations from Khosronejad et al. [14], Froehlich [26], and Mussetter et al. [28] tend to overestimate scour, as they exceed the initially proposed value for the MNE. On the other hand, although the Pereira [33] and Borges [23] equations deliver MNE values within the suggested range, their results tend to underestimate the calculated scour.

Table 2. Statistical estimators were obtained by comparing experimental measurements with the prediction equations.

MNE	*MPF*	*MSE* (mm^2)	*RMSE* (mm)	Equation	Reference
63.03	4.67	0.0015	0.0381	Lischtvan-Lebediev	[19]
219.54	2.78	0.0024	0.0485	Froehlich	[26]
170.53	2.11	0.0012	0.0353	Pereira	[33]
110.41	2.93	0.0053	0.0690	Borges	[23]
1816.46	3.20	0.0038	0.0619	Mussetter	[28]
201.93	3.06	0.0023	0.0483	Khosronejad et al.	[14]
68.72	3.60	0.0010	0.0321	Proposed equation	This research

As proposed by Aguirre-Pe [38], an acceptable limit for MPF is 12 was established. Accordingly, the MPF values obtained for each equation tend to overestimate the MPF value; thus, there is a wide dispersion in the relations between the observed and the calculated values. The closest equation is the one described by Pereira [33], with a difference of 1.49 compared to the proposed equation. In the case of the MSE and the RMSE, a value of 0 is ideal as it would represent an optimal model. The proposed equation delivers better performance with MSE = 0.001 mm^2, and $RMSE$ = 0.032 mm.

4. Conclusions

The proposed equation considers conditions other researchers have not considered, such as the condition of a well-graded granular bed, longitudinal walls, and wall embedment. The experimental models have identified the slope and flow rate as the most influential variables in the local scouring of longitudinal walls. An increase in these parameters during the experiments resulted in exponential growth in local scour. It is essential to highlight that only the Lischtvan–Lebediev equation tends to estimate measured scour more accurately, and it is observed that the Mussetter, Froehlich, and Khosronejad equations overestimate scour. At the same time, those proposed by Borges and Pereira underestimate scour. Finally, the validation of the equations employing statistical estimators shows that, in comparison with the other equations, the equation proposed in this research presents improvements in most of the validated statistical estimators; however, it is necessary to confront the resolution capacity of this new equation with experimental data under natural conditions.

Author Contributions: Conceptualization, G.A.C.S. and A.G.C.; methodology, A.G.C. and N.J.C.C.; software, N.J.C.C.; validation, N.J.C.C., G.A.C.S. and A.G.C.; formal analysis, N.J.C.C.; investigation, N.J.C.C.; resources, G.A.C.S. and A.G.C.; data curation, G.A.C.S. and A.G.C.; writing—original draft preparation, N.J.C.C.; writing—review and editing, G.A.C.S. and A.G.C.; visualization, N.J.C.C.; supervision, G.A.C.S. and A.G.C.; project administration, G.A.C.S. and A.G.C.; funding acquisition, G.A.C.S., N.J.C.C. and A.G.C. All authors have read and agreed to the published version of the manuscript.

Funding: This research was funded by the program for the doctoral formation of Universidad Francisco de Paula Santander.

Data Availability Statement: Data are contained within the article.

Acknowledgments: The authors sincerely thank Universidad Santo Tomás (Tunja, Colombia) for the opportunity to experiment. We also thank Universidad del Valle and Universidad Francisco de Paula Santander for their technical and administrative support.

Conflicts of Interest: The authors declare no conflict of interest.

Appendix A

Calculation of α and β coefficients.

$$\alpha = \frac{Q_d}{Y_m^{1/453}\ B_e} \tag{A1}$$

where α = Section coefficient, Q_d = Design flow associated with the return period, $Y_m^{\frac{5}{3}}$ = Mean depth of flow, and B_e = Effective section width.

$$\beta = 0.7929 + 0.0973\ Ln(T) \tag{A2}$$

where β = frequency coefficient, and T = Return period selected for the design ranging from 15 to 1500 years.

Table A1. χ values for cohesive and non-cohesive soils.

Cohesive Soils			**Non-Cohesive Soils**		
γ_m **(mm)**	χ	**1/(1+χ)**	***d*** **(mm)**	χ	**1/(1+χ)**
0.80	0.52	0.66	0.05	0.43	0.70
0.83	0.51	0.66	0.15	0.42	0.70
0.86	0.50	0.67	0.50	0.41	0.71
0.88	0.49	0.67	1.00	0.40	0.71
0.90	0.48	0.67	1.50	0.39	0.72
0.93	0.47	0.68	2.50	0.38	0.72
0.96	0.46	0.68	4.00	0.37	0.73
0.98	0.45	0.69	6.00	0.36	0.74
1.00	0.44	0.69	8.00	0.35	0.74
1.04	0.43	0.70	10.00	0.34	0.75
1.08	0.42	0.70	15.00	0.33	0.75
1.12	0.41	0.71	20.00	0.32	0.76
1.16	0.40	0.71	25.00	0.31	0.76
1.20	0.39	0.72	40.00	0.30	0.77
1.20	0.38	0.72	60.00	0.29	0.78
1.28	0.37	0.73	90.00	0.28	0.78
1.34	0.36	0.74	140.00	0.27	0.79
1.40	0.35	0.74	190.00	0.26	0.79
1.46	0.34	0.75	250.00	0.25	0.80
1.52	0.33	0.75	310.00	0.24	0.81
1.58	0.32	0.76	370.00	0.23	0.81
1.64	0.31	0.76	450.00	0.22	0.83
1.71	0.30	0.77	570.00	0.21	0.83
1.80	0.29	0.78	750.00	0.20	0.83
1.89	0.28	0.78	1000.00	0.19	0.84
2.00	0.27	0.79			

References

1. Czapiga, M.J.; Blom, A.; Viparelli, E. Efficacy of Longitudinal Training Walls to Mitigate Riverbed Erosion. *Water Resour. Res.* **2022**, *58*, e2022WR033072. [CrossRef]
2. Yan, G.; Cheng, H.; Jiang, Z.; Teng, L.; Tang, M.; Shi, T.; Jiang, Y.; Yang, G.; Zhou, Q. Recognition of Fluvial Bank Erosion Along the Main Stream of the Yangtze River. *Engineering* **2022**, *19*, 50–61. [CrossRef]
3. Sohrabi, M.; Keshavarzi, A.; Javan, M. Impact of Bed Sill Shapes on Scour Protection in River Bed and Banks. *Int. J. River Basin Manag.* **2019**, *17*, 277–287. [CrossRef]
4. Shahriar, A.R.; Ortiz, A.C.; Montoya, B.M.; Gabr, M.A. Bridge Pier Scour: An Overview of Factors Affecting the Phenomenon and Comparative Evaluation of Selected Models. *Transp. Geotech.* **2021**, *28*, 100549. [CrossRef]
5. Qi, H.; Yuan, T.; Zhao, F.; Chen, G.; Tian, W.; Li, J. Local Scour Reduction around Cylindrical Piers Using Permeable Collars in Clear Water. *Water* **2023**, *15*, 897. [CrossRef]
6. Le, T.B.; Crosato, A.; Uijttewaal, W.S.J. Long-Term Morphological Developments of River Channels Separated by a Longitudinal Training Wall. *Adv. Water Resour.* **2018**, *113*, 73–85. [CrossRef]

7. Toapaxi, J.; Galiano, L.; Castro, M.; Hidalgo, X.; Valencia, N. Análisis de La Socavación En Cauces Naturales. *Rev. Politec.* **2015**, *35*, 1–11.
8. Kokusho, T.; Hara, T.; Hiraoka, R. Undrained Shear Strength of Granular Soils with Different Particle Gradations. *J. Geotech. Geoenvironmental Eng.* **2004**, *130*, 621–629. [CrossRef]
9. Biron, P.M.; Robson, C.; Lapointe, M.F.; Gaskin, S.J. Three-Dimensional Flow Dynamics around Deflectors. *River Res. Appl.* **2005**, *21*, 961–975. [CrossRef]
10. Istanbulluoglu, E.; Tarboton, D.G.; Pack, R.T.; Luce, C. A Sediment Transport Model for Incision of Gullies on Steep Topography. *Water Resour. Res.* **2003**, *39*, 4. [CrossRef]
11. Attal, M.; Lavé, J. Pebble Abrasion during Fluvial Transport: Experimental Results and Implications for the Evolution of the Sediment Load along Rivers. *J. Geophys. Res.* **2009**, *114*, F04023. [CrossRef]
12. Barbosa Gil, S. Metodología Para Calcular La Profundidad de Socavación General En Ríos de Montaña (Lecho de Gravas). Ph.D. Thesis, Universidad Nacional de Colombia, Bogota, Colombia, 2013.
13. Cañas, R. Estudio de La Socavación Local En Pilas Circulares de Puentes En Lechos No Cohesivos Con Modelación Física En Laboratorio. Master's Thesis, Escuela Colombiana de Ingenieria Julio Garavito, Bogota, Colombia, 2018.
14. Khosronejad, A.; Diplas, P.; Angelidis, D.; Zhang, Z.; Heydari, N.; Sotiropoulos, F. Scour Depth Prediction at the Base of Longitudinal Walls: A Combined Experimental, Numerical, and Field Study. *Environ. Fluid Mech.* **2020**, *20*, 459–478. [CrossRef]
15. Taha, N.; El-Feky, M.M.; El-Saiad, A.A.; Fathy, I. Numerical Investigation of Scour Characteristics Downstream of Blocked Culverts. *Alex. Eng. J.* **2020**, *59*, 3503–3513. [CrossRef]
16. Johnson, P.A.; Clopper, P.E.; Zevenbergen, L.W.; Lagasse, P.F. Quantifying Uncertainty and Reliability in Bridge Scour Estimations. *J. Hydraul. Eng.* **2015**, *141*, 04015013. [CrossRef]
17. Lacey, G. Stable channels in alluvium (includes appendices). *Minutes Proc. Inst. Civ. Eng.* **1930**, *229*, 259–292. [CrossRef]
18. Blench, T. A new theory of turbulent flow in liquids of small viscosity. (in abstract form). *J. Inst. Civ. Eng.* **1939**, *11*, 611–612. [CrossRef]
19. Lischtvan, L.; Lebediev, V. Gidrologia I Gidraulika v Mostovom Doroshnom, Straitielvie. In *Hydrology and Hydraulics in Bridge and Road Building*; Gidrometeoizdat: St. Petersburg, Russian, 1959.
20. Laursen, E.M.; Toch, A. *Bulletin no Scour around Bridge Piers and Abutments Iowa Institute of Hydraulic Research in Cooperation with Thl Iowa State Highway Commission and the Bureau of Public Roads*; Iowa Highway Research Board: Ames, IA, USA, 1956.
21. Straub, L.G. Report of Committee on Dynamics of Streams, 1937–1938. *Trans. Am. Geophys. Union* **1938**, *19*, 349. [CrossRef]
22. Komura, S. Equilibrium Depth of Scour in Long Constrictions. *J. Hydraul. Div.* **1966**, *92*, 17–37. [CrossRef]
23. Borges, M. Socavacion al Pie de Muros Longitudinales. Bachelor's Thesis, Universidad de Merida, Merida, Mexico, 2008.
24. Richardson, E.V.; Simons, D.B.; Julien, P.Y. *Highways in the River Environment: Participant Notebook*; Federal Highway Administration: Washington, DC, USA, 1990.
25. Melville, B.W. Pier and Abutment Scour: Integrated Approach. *J. Hydraul. Eng.* **1997**, *123*, 125–136. [CrossRef]
26. Froehlich, D.C. Local Scour at Bridge Abutments. In Proceedings of the 1989 National Conference on Hydraulic Engineering, ASCE, New Orleans, LA, USA, 14 August 1989; pp. 13–18.
27. Melville, B.W. Local Scour at Bridge Abutments. *J. Hydraul. Eng.* **1992**, *118*, 615–631. [CrossRef]
28. Mussetter, B.; Stoliker, D.; Foglesong, R.; Alsop, T.; Aguirre, F.; Stone, H.; Dodge, C.; Mortenson, J.; Carroll, R. Sediment and Erosion Design Guide Sscafca Sediment and Erosion Design Guide. 2008. Available online: https://sscafca.org/development/documents/sediment_design_guide/Sediment%20Design%20Guide%2012-30-08.pdf (accessed on 7 November 2023).
29. Look, B.G. *Handbook of Geotechnical Investigation and Design Tables*; Taylor & Francis: Oxfordshire, UK, 2007; ISBN 9780429224379.
30. Chachereau, Y.; Chanson, H. Free-Surface Fluctuations and Turbulence in Hydraulic Jumps. *Exp. Therm. Fluid Sci.* **2011**, *35*, 896–909. [CrossRef]
31. Guzmán, R.; Bezada, M.; Rodríguez-Santalla, I. Granulometric Characterization of Sediments in the Anastomosed System of the Apure River Venezuela. *J. S. Am. Earth Sci.* **2021**, *109*, 103274. [CrossRef]
32. Khan, U.A.; Valentino, R. Investigating the Granulometric Distribution of Fluvial Sediments through the Hybrid Technique: Case Study of the Baganza River (Italy). *Water* **2022**, *14*, 1511. [CrossRef]
33. Pereira, L.M. Erosión Local En Estribos. Master's Thesis, Universidad de los Andes, Merida, Mexico, 1995.
34. Gonzalez, J.R.P.; Escobar-Vargas, J.; Vargas-Luna, A.; Castiblanco, S.; Trujillo, D.; Guatame, A.C.; Corzo, G.; Santos, G.; Perez, L.A. Hydroinformatic Tools and Their Potential in the Search for Missing Persons in Rivers. *Forensic Sci. Int.* **2022**, *341*, 111478. [CrossRef] [PubMed]
35. Oliveto, G.; Hager, W.H. Temporal Evolution of Clear-Water Pier and Abutment Scour. *J. Hydraul. Eng.* **2002**, *128*, 811–820. [CrossRef]
36. Di Pietro, P.; Mahajan, R.R. *Erosion Control Solutions with Case Studies*; Springer: Berlin/Heidelberg, Germany, 2022; pp. 71–94.
37. Radice, A.; Davari, V. Roughening Elements as Abutment Scour Countermeasures. *J. Hydraul. Eng.* **2014**, *140*, 06014014. [CrossRef]
38. Aguirre-Pe, J.; Olivero, M.L.; Moncada, A.T. Particle Densimetric Froude Number for Estimating Sediment Transport. *J. Hydraul. Eng.* **2003**, *129*, 428–437. [CrossRef]